Use of a hydrologic mixing model to examine the roles of meltwater, precipitation and groundwater in the Langtang River basin, Nepal

Alāna M. WILSON,[1,2] Mark W. WILLIAMS,[1,2] Rijan B. KAYASTHA,[3] Adina RACOVITEANU[4]

[1]*Institute of Arctic and Alpine Research, University of Colorado Boulder, Boulder, CO, USA*
[2]*Department of Geography, University of Colorado Boulder, Boulder, CO, USA*
[3]*Department of Environmental Science and Engineering, School of Science, Kathmandu University, Kathmandu, Nepal*
[4]*National Snow and Ice Data Center, University of Colorado Boulder, Boulder, CO, USA*
Correspondence: Alāna M. Wilson <alana.wilson@colorado.edu>

ABSTRACT. Understanding the hydrology of glacierized catchments is an important step in assessing the vulnerability of water resources to a changing climate. While there have been increased efforts recently to understand the dynamics of Asia's cryosphere, glacier melt dynamics and hydrograph separation of river discharge are open questions. A multi-year, multi-seasonal dataset of water chemistry from the Langtang Valley, Nepal, is used to explore water sources and flow paths that contribute to Langtang River discharge. Differences in hydrochemistry of samples from debris-free Khimsung Glacier and debris-covered Lirung Glacier demonstrate the effect of debris cover on glacier outflow. Additional data show seasonal transitions in the composition of Langtang River discharge. End-member mixing analysis (EMMA) using geochemical and isotopic tracers suggests that reacted meltwater contributes the majority of flow during most of the year, with the exception of the summer when unreacted meltwater and precipitation dominate streamflow. We hypothesize our dataset is missing characteristic monsoon water and utilize a Late May river sample as a proxy for precipitation-influenced groundwater in the EMMA. Results offer insight into the plausibility of flow sources and pathways in the basin.

KEYWORDS: debris-covered glaciers, meltwater chemistry, mountain glaciers

1. OVERVIEW

Snow and glaciers of High Mountain Asia are the source of water for much of the continent's population (Immerzeel and others, 2010). The hydrology of high-elevation, glacierized catchments is influenced by local precipitation patterns, and snow and ice melt regimes; little is known about the role of groundwater (La Frenierre and Mark, 2014). In South Asia, monsoon activity strongly influences the timing of precipitation, as well as the energy balance of glaciers and snowpack (Sakai and others, 1998; Baral and others, 2014). Debris cover can be extensive on glacier tongues and enhance or inhibit melt, depending on thickness, further confounding our understanding of glacial hydrology (Kayastha and others, 2000).

As glaciers retreat and precipitation changes from snow to rain, the hydrographs in snow- and ice-covered catchments will change. Glacierized catchments like the Langtang Valley, Nepal, have the potential to transition to a snowmelt- and rainfall-dominated hydrograph, which could reduce peak discharge in late summer relative to present-day values which are influenced by late-summer glacier melt (Immerzeel and others, 2012). For downstream water managers, understanding magnitudes and seasonal shifts in the hydrograph has profound implications (e.g. for diversions and reservoir levels). Water balance, the net movement of water in or out of a system, is often difficult to quantify at the basin scale. The remote and rugged terrain of the Himalaya makes it a data-poor region with respect to traditional ground-based glaciological (UNEP and WGMS, 2008) and hydrometeorological (Chalise and others, 2003) measurements. Remote sensing faces challenges closing the water balance, and field measurements may not be representative when extrapolated over large areas (Zemp and others, 2009; Nepal and others, 2014). Hydrochemistry-based mixing models offer an alternative to these methods by utilizing naturally occurring tracers to estimate proportions of river discharge from various sources and flow paths (La Frenierre and Mark, 2014).

Measurement of geochemical species in water samples differentiates them into two primary categories: 'reacted' waters and 'unreacted' waters (Sueker and others, 2001). Reacted waters typically travel in the subsurface and acquire elevated solute levels via processes such as ion exchange and mineral weathering. In glacierized catchments this increase in concentration of chemical tracers can also occur with flow at the bedrock interface, through moraines or through glacial till, and depends on length of contact with solute sources. Surface waters that have not undergone any infiltration, such as some snowmelt and glacier ice melt, typically have low solute concentrations and are considered unreacted waters.

Isotopic tracers, in contrast to geochemical tracers, are not influenced by flow path unless evaporation occurs, but they can potentially provide useful information on the location or timing of the original precipitation source (Hooper and Shoemaker, 1986). The ^{18}O isotope in water is

https://doi.org/10.3189/2016AoG71A067 Published online by Cambridge University Press

known to become more depleted with lower temperatures, higher elevations and distance from moisture source (Poage and Chamberlain, 2001). This affects the seasonal variability of isotope values in precipitation and helps differentiate sources of streamflow.

Hydrologic mixing models utilize the distinctive chemistry of different end-member sources (e.g. snowmelt, glacier melt, groundwater, rain) to quantify their contribution to total discharge. Discharge data are not required as the hydrograph separation estimates proportional contributions that come from each end-member (Liu and others, 2004), which makes them particularly strategic for poorly monitored glacierized catchments (Barthold and others, 2010). Mixing-model results may also provide insight into how the timing and volume of discharge may change in response to changes in climate (Kong and Pang, 2012). Hydrologic mixing models have not been applied extensively in Himalayan catchments. Racoviteanu and others (2013) demonstrate that utilizing $\delta^{18}O$ as a sole tracer produces plausible results separating groundwater from snow and ice melt in the Langtang River basin, results which are comparable to estimates they found using an elevation-dependent ice ablation model derived from remote-sensing data. In the pre-monsoon season from March to May, Bookhagen (2012) reports that snowmelt is the most important water source in the central Himalayan region, with rainfall and glacier melt becoming prominent in the summer months. The role of groundwater in glacierized catchments is poorly known (Nepal and others, 2014), though at the mountain-front scale in Nepal it is estimated to contribute approximately two-thirds to total discharge of the country's rivers (Andermann and others, 2012). La Frenierre and Mark (2014) highlight the need for hydrograph separation to be conducted at the scale of individual catchments to assess variability across a region, and they underscore the need for exploring the relationship between glacier melt and groundwater systems.

The hydrochemistry dataset presented here is used to assess the flow paths and seasonal shifts in hydrology of the glacierized Langtang Valley, and offers one of the first quantitative evaluations of subsurface flow in the basin. End-member mixing analysis (EMMA) is utilized for synoptic water samples from multiple years in different seasons. Given that mass loss of debris-covered glaciers in the Langtang basin happens predominantly through downwasting and Lirung Glacier is estimated to be retreating at $\sim 5\,m\,a^{-1}$ (Pellicciotti and others, 2015), the consideration of samples spanning the 2008–13 time frame is not likely to be affected by changes in glacier area, though interannual variability is a factor in precipitation volume and timing, and in runoff. We also investigate whether the content of meltwater differs between debris-covered and debris-free glaciers, and if so, whether that helps in separating the mass contribution from these two glacier types to river flow.

We hypothesize that outflow from glaciers in the pre-monsoon is primarily unreacted snowmelt and the composition transitions to debris-influenced ice-melt (reacted-water) dominance in the post-monsoon. Concentrations of solutes are expected to increase with distance downstream from the glaciers, and are expected to be higher in the post-monsoon season datasets versus the pre-monsoon samples collected during the spring snowmelt. A precipitation signal is expected along the entire elevational gradient both during the summer and through the fall, as some precipitation experiences delayed flow through the subsurface.

2. FIELD AREA

Fieldwork was conducted in the Langtang Valley of Nepal's central-eastern Himalaya (Fig. 1), part of Langtang National Park, 60 km north of Kathmandu. The basin is defined upstream of the confluence of the Langtang River and Trishuli River, at 1460 m at the town of Syafrubensi. The highest point in the catchment is Langtang Lirung's 7246 m summit. The Langtang basin is in the headwaters of the Trishuli basin, which flows into the Narayani basin, a tributary of the River Ganga. The basin at Syafrubensi is $585\,km^2$ in area and at least 23% glacierized (Motoyama and Yamada, 1989). Pleistocene glaciation extended down to an elevation of 3011 m, depositing unconsolidated glacial sediments which suggest the opportunity for enhanced groundwater retention over a large swath of the basin above 3011 m (Barnard and others, 2006). Based on field observations, the treeline is estimated to be at 3100 m on the north side of the valley and at 3900 m on the south side of the valley.

Geologically, the catchment is part of the Miocene High Himalayan granite association (Inger and Harris, 1993) and exposed bedrock is typically gneiss, leucogranite and migmatites (Schramm and others, 1998). The valley is east–west-trending and the western end of the valley is along the Main Central Thrust intracontinental subduction zone of the Himalaya (MacFarlane, 1993). MacFarlane also mapped lithologic units on the north side of the Langtang Valley (the side accessible by trail): various gneiss units, granite and landslide deposits.

The upper Langtang basin ($\sim 350\,km^2$) is defined upstream of a Nepali Department of Hydrology and Meteorology (DHM) gauging station at 3642 m (R4 in Fig. 1). Ice-covered area estimates for the upper basin range from 38% to 46% (Motoyama and Yamada, 1989; Immerzeel and others, 2012). Langtang Glacier is the largest glacier in the catchment at $\sim 75\,km^2$ (Wagnon and others, 2007) and outflow from its terminus is the origin of the Langtang River. The Lirung sub-basin (Fig. 2), part of the upper basin, contains debris-covered Lirung Glacier ($7.2\,km^2$) and debris-free Khimsung Glacier ($4.2\,km^2$). The upper basin's discharge follows that of a glacial regime, with the maximum discharge in late summer coinciding with both glacier melt and monsoon precipitation, followed by base flow on the recession in the winter (Immerzeel and others, 2012). Based on gauging-station data, flow out of the upper basin ranges from 3 to $16\,m^3\,s^{-1}$ throughout the year (Racoviteanu and others, 2013). Glacio-hydrological observations in the Langtang Valley have been conducted since 1981 (Higuchi, 1993).

The location of the Langtang Valley in the central-eastern Himalaya gives it a monsoon-dominated climate and precipitation regime. Annual precipitation measured by DHM averages $622\,mm\,a^{-1}$ at the Kyangjing meteorological station (3924 m), with ~80% falling between May and September (Barnard and others, 2006). Snow accumulation and melt patterns are thus driven in part by monsoon-season moisture, temperatures and cloud cover, and the region's glaciers have been designated 'summer-accumulation' type (Ageta and Higuchi, 1984). Normal monsoon onset in the region is ~10 June and retreat is ~20 September according to DHM records. The elevation of maximum precipitation during the monsoon is near 2500 m (Baral and others, 2014). Barnard and others (2006) reported the equilibrium-line altitude (ELA) of glaciers in the valley to be 5320 m,

https://doi.org/10.3189/2016AoG71A067 Published online by Cambridge University Press

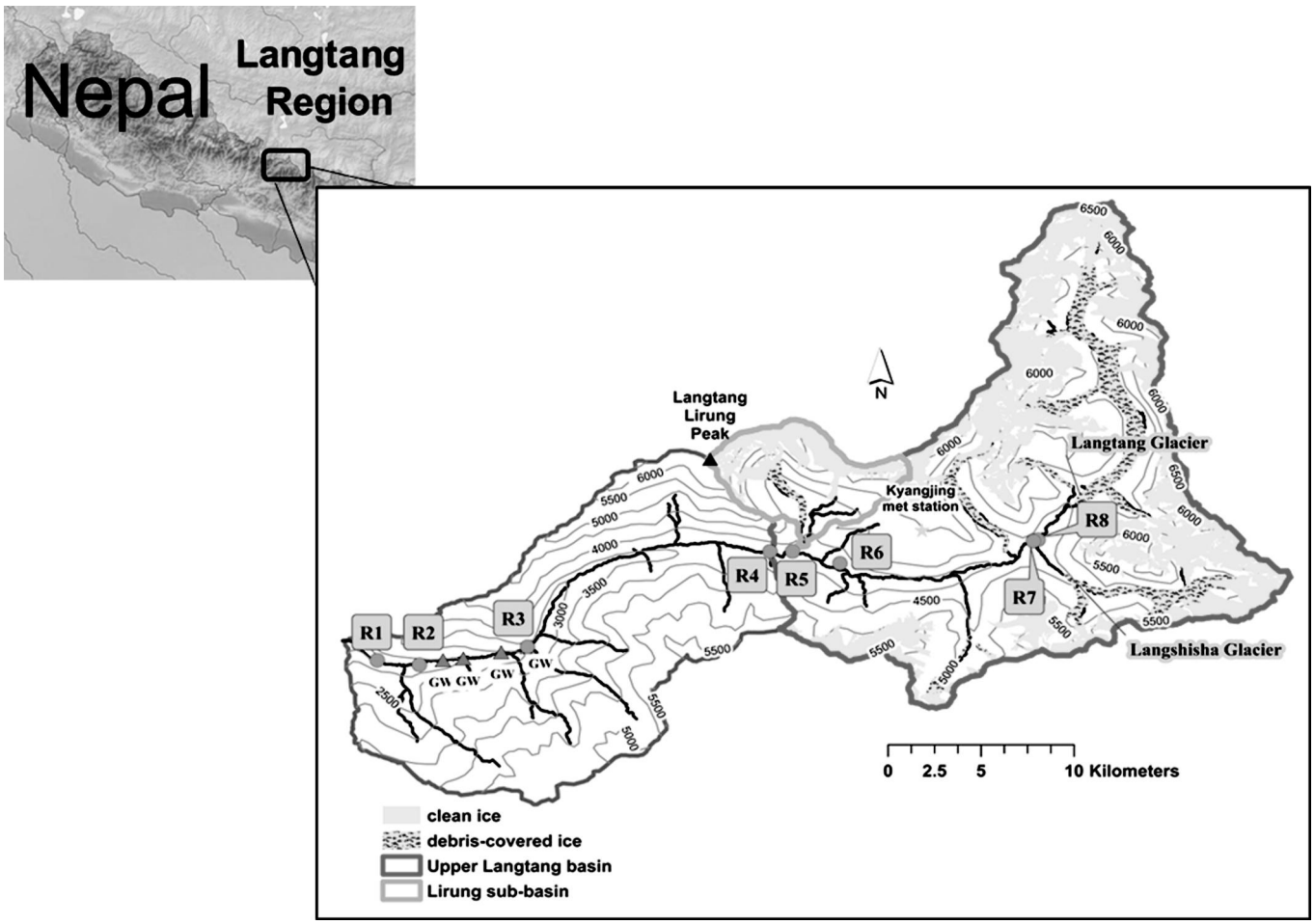

Fig. 1. Overview of Langtang Valley location in the Nepalese Himalaya and sampling locations along the Langtang River (R1–R8) and groundwater springs (GW). Upper Langtang basin and Lirung sub-basin are delineated.

indicating that a large portion of the upper Langtang basin receives monsoon precipitation in the form of snow, contributing to the long-term survival of its glaciers.

3. METHODS

3.1. Sample collection

Samples used for analysis were collected during three field campaigns: October 2008 (isotopic values reported by Racoviteanu and others, 2013), the pre-monsoon season of May 2012 and the post-monsoon season of October/November 2013. The May 2012 samples were collected during two separate synoptic surveys and are identified as 'Early May' and 'Late May'. Two sets of samples, one geochemical and one isotopic, were collected during each campaign from Langtang River streamwater along an elevational gradient and from various sources that contribute to river discharge (Table 1). Some sites were only sampled during one season.

Sampling locations visited in both seasons included a transect along the Langtang River, groundwater springs and glacier sites in the Lirung sub-catchment. Five Langtang River sites were sampled along an elevational gradient from Syafrubensi (1479 m) to Kyangjing (3745 m), upstream of the confluence with the Lirung sub-catchment. Four springs (1868–2539 m) were sampled to characterize groundwater. These springs are well below the glaciated terrain of the upper Langtang basin. Outflow from Lirung Glacier (3784 m) and Khimsung Glacier (4166 m) was sampled to represent meltwater from debris-covered and debris-free glaciers, respectively. Supraglacial water was collected from the surface of Lirung Glacier (4041–4110 m). Sampling locations visited in only one season included three sites along the

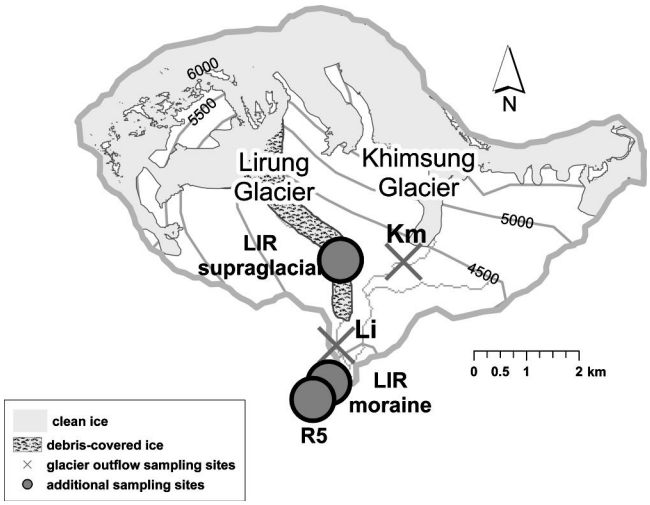

Fig. 2. Lirung sub-basin sampling locations, including the R5 Langtang River site just above the confluence of the Lirung outlet and the Langtang River.

https://doi.org/10.3189/2016AoG71A067 Published online by Cambridge University Press

Table 1. Locations and timing of Langtang River water and its end-members, and median values of oxygen-18 isotope data

Site name	Description	Site code	# pre-monsoon samples (2012)	# post-monsoon samples (2013)	Elevation	Pre-monsoon $\delta^{18}O$ (median)	Post-monsoon $\delta^{18}O$ (median)
					m	‰	‰
Langtang River near Syafrubensi*	River	R1	3	2	1479	–13.19	–14.27
Langtang River at landslide*	River	R2	1	3	1680	–13.77	–14.72
Langtang River at Lama Hotel*	River	R3	1	6	2427	–14.43	–15.06
Langtang River at DHM gauge	River	R4	2	3	3642	–11.83	–15.83
Langtang River at Kyangjing*	River	R5	4	2	3745	–12.14	–16.33
Langtang River, upstream Yala Glacier	River	R6	0	1	3950	–12.32	–15.83
Langtang River, downstream Langshisha	River	R7	0	2	4070	–12.47	–17.49
Langtang River, upstream Langshisha	River	R8	0	1	4121	–12.88	–17.37
Rain	End-member	Rn	2	0	3880	–3.80	–
Snow	End-member	sn	3	2	4166–5268	–7.25	–17.89
Groundwater	End-member	gw	4	10	2001–3319	–12.29	–13.25
Khimsung Glacier outflow	End-member	Km	36	6	4166	–13.80	–15.94
Lirung Glacier outflow	End-member	Li	22	12	3784	–10.42	–15.47
Lirung Glacier ice	End-member	LiI	0	2	4102–4235	–	–15.93
Lirung moraine seepage	End-member	LiM	8	0	3794–3796	–14.09	–
Lirung supraglacial	End-member	LiS	5	1	4041–4110	–11.77	–18.78
Langtang Glacier outflow	End-member	Lng	0	2	4505	–	–17.23
Langtang Glacier ice	End-member	LngI	0	1	4507	–	–16.14
Langshisha Glacier outflow	End-member	Lsh	0	4	4171	–	–17.67

*Additional October 2008 Langtang River sample.

Langtang River above Kyangjing, outflow from Langtang Glacier (4505 m), outflow from Langshisha Glacier (4171 m), outflow seeping from the Lirung terminal moraine (3794 m), and ice samples from Lirung and Langtang Glaciers. Lirung, Langtang and Langshisha glaciers have debris-covered tongues. Pre-monsoon rain was collected during a single precipitation event in the village of Kyangjing on 11 May 2012. Snow samples (4166–5268 m) were collected in both seasons but at elevations >1000 m apart.

For a 72 hour window from 6 to 9 May (days of year 127–130), automatic samplers were used to collect water samples every 2 hours from Lirung Glacier outflow and Khimsung Glacier outflow. These samples allowed us to compare the geochemistry and isotopic profiles of meltwater from debris-covered and debris-free glaciers. Elevation of the snowline during the high-frequency sampling was estimated at 4700 m.

Sampling protocols followed those developed by the Niwot Ridge Long Term Ecological Research program for high-elevation catchments (Williams and others, 2006). Surface waters were collected as grab samples. Pre-monsoon snow was collected as a 1 m depth-integrated core on Yala Glacier, and post-monsoon snow samples were collected from fresh snowfall near the terminus of Langtang Glacier and depth-integrated over <0.5 m. Ice samples were collected from ice faces on the terminus of Lirung and Langtang Glaciers and intentionally excluded surface debris. All samples for geochemical analysis were collected in polyethylene bottles which were soaked overnight and rinsed three times with deionized water, then rinsed three times with filtered sample water before sample collection. All geochemical samples were filtered in the field within 24 hours of collection using 1.2 µm glass microfiber filters. Snow and ice samples were allowed to melt at ambient temperature and were filtered within 24 hours of melt. Isotopic samples were filtered and stored in 25 mL glass vials with TaperSeal™ caps.

3.2. Laboratory analysis

Samples from all field campaigns were analyzed at the Kiowa Wet Chemistry Laboratory, Institute of Arctic and Alpine Research, Boulder, CO, USA, for Ca^{2+}, Mg^{2+}, Na^{+}, K^{+}, Cl^{-}, SO_4^{2-} and oxygen and hydrogen isotopes of the water molecule (^{18}O and deuterium ($^{2}H = D$)). Detection limits for all major solutes were <0.2 µEq L^{-1}. Isotopic analysis was conducted using wavelength-scanned cavity ringdown spectroscopy (WS-CRDS). Deuterium excess (d-excess) was calculated from the relationship between $\delta^{18}O$ and δD using the equation developed by Johnsen and others (1989). All values are reported in µEq L^{-1} except for the isotopes, which use the standard delta (δ) notation as parts per thousand (‰) in their deviation from Vienna Standard Mean Ocean Water (VSMOW) with a precision of ±0.05‰ for both δD and $\delta^{18}O$.

3.3. Hydrograph separation model

Hydrologic mixing models determine proportions of flow coming from different sources without predetermining what those sources are. The presence of multiple sources, or end-members, can be tested and a suite of chemistry data can be used to identify end-members which best explain the chemistry of river streamflow. EMMA (Christophersen and others, 1990; Hooper and others, 1990) allows for the inclusion of an unlimited number of geochemical and isotopic tracers by reducing the dimensionality of the streamwater data with principal component analysis (PCA). EMMA can consider numerous end-members by plotting end-member chemistry relative to streamwater samples in dimensions defined by the principal components retained from the PCA. Projection of the chemistry data into PCA space produces an EMMA with one more end-member component than the number of principal components used. For example a three-component EMMA is generated using two principal components.

https://doi.org/10.3189/2016AoG71A067 Published online by Cambridge University Press

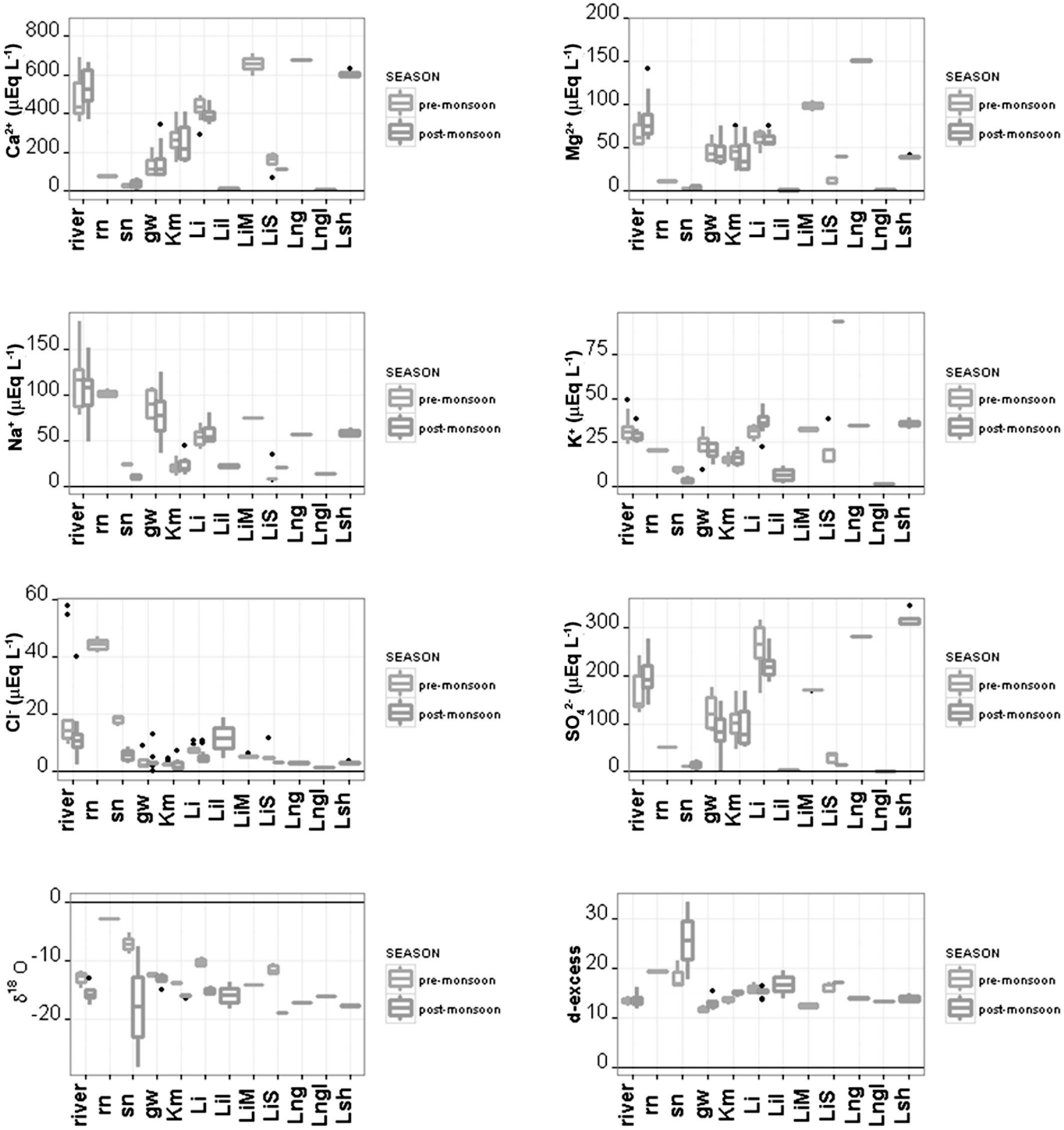

Fig. 3. Boxplots comparing pre-monsoon (May 2012) and post-monsoon (October/November 2013) values of geochemical (µEq L^{-1}) and isotopic tracers (‰) in Langtang River water and its end-members: rain (rn), snow (sn), groundwater (gw), Khimsung Glacier (Km), Lirung Glacier (Li), Lirung Glacier ice (LiI), Lirung moraine (LiM), Lirung supraglacial (LiS), Langtang Glacier (Lng), Langtang Glacier ice (Lngl), Langshisha Glacier (Lsh).

EMMA was conducted to identify the source waters that contribute to Langtang River discharge seasonally and along an elevation gradient. Conservative geochemical and isotopic tracers were determined following Hooper (2003). Hooper (2003) used statistical diagnostic tools to assess conservative behavior of tracers and evaluate how well the multivariate stream chemistry data are explained by a given number of principal components. Proportions of flow were assigned to end-members using a least-squares method to select those that best explain the streamwater chemistry (Christophersen and Hooper, 1992). The final calculation of fractional contribution, as illustrated for three end-members, is

$$SW_{U1} = \alpha_1 EM_{1U1} + \alpha_2 EM_{2U1} + \alpha_3 EM_{3U1} \quad (1)$$

$$SW_{U2} = \alpha_1 EM_{1U2} + \alpha_2 EM_{2U2} + \alpha_3 \quad (2)$$

where α_1, α_2 and α_3 are the fractions of each end-member based on Euclidean distance from a streamwater sample to each end-member, SW_{U1} and SW_{U2} are the projected

https://doi.org/10.3189/2016AoG71A067 Published online by Cambridge University Press

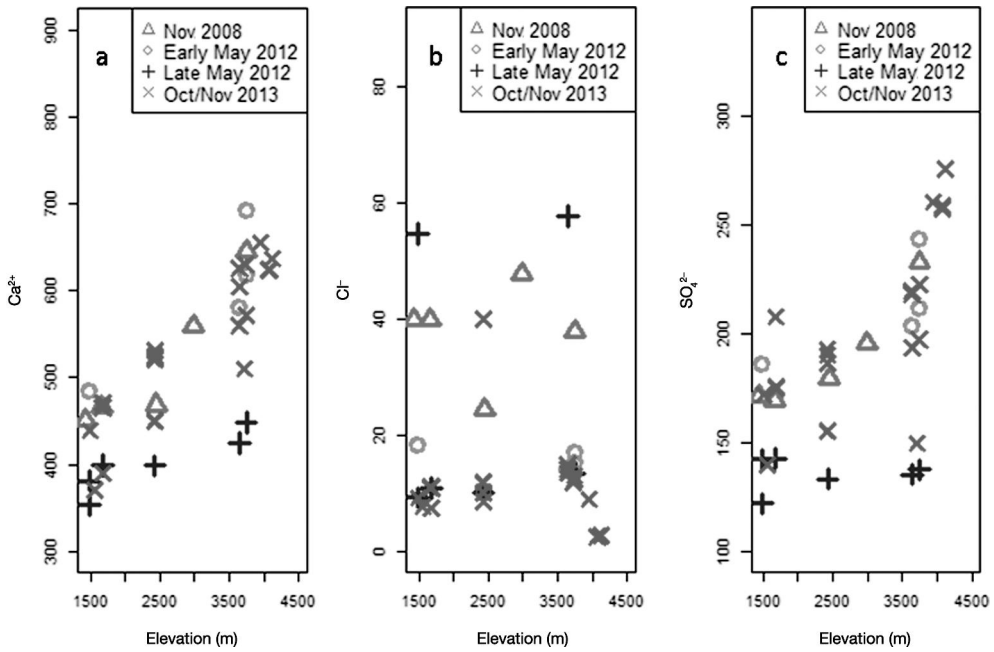

Fig. 4. Trends in Langtang River water chemistry (μEq L^{-1}) by season.

streamwater values in PCA space, and EM_{nU1} and EM_{nU2} are the coefficients of the *n*th end-member projected in PCA space (Christophersen and others, 1990; Liu and others, 2004; Barthold and others, 2010).

4. RESULTS

4.1. Chemistry and isotopic tracers

Precipitation and ice samples exhibited concentrations of solutes which were consistently low with the exception of sodium and chloride (Fig. 3). Ice samples ($n = 3$) generally had solute concentrations <5 μEq L^{-1}. Maximum solute concentrations for ice were <25 μEq L^{-1} and <70 μEq L^{-1} for snow. Pre-monsoon rain ($n = 2$) had elevated sodium (107 μEq L^{-1}) and chloride (47 μEq L^{-1}) concentrations, so these tracers were not associated with post-depositional processes. The sodium and chloride values for rain were about five times the median values for glacier ice and snow. Both pre-monsoon snow ($n = 3$) and post-monsoon snow ($n = 2$) had sodium and chloride concentrations <25 μEq L^{-1}. The high correlation coefficient between sodium and chloride in ice and precipitation samples (0.92, $n = 10$) dropped to 0.54 ($n = 152$) when all samples were considered.

Lirung Glacier outflow, Lirung moraine seepage, Langtang Glacier outflow and Langshisha Glacier outflow all contain elevated concentrations of calcium (>350 μEq L^{-1}), magnesium (>39 μEq L^{-1}) and sulfate (>170 μEq L^{-1}) when compared to values in rain, snow and ice (Fig. 3). These elevated concentrations suggest post-precipitation processes associated with reacted waters, and differentiate these end-members from unreacted waters. Rain, snow, Khimsung Glacier outflow, glacier ice and Lirung supraglacial water have relatively lower calcium, magnesium and sulfate values, indicating limited interaction with rock or sediments and leaving them with the chemical signature of unreacted waters. Groundwater samples from the low-elevation springs had intermediate values of these tracers.

There was a large range in the isotopic values of both precipitation and surface waters. The $\delta^{18}O$ values in precipitation ranged from a post-monsoon snow value of –28.1‰ to –2.8‰ in pre-monsoon rain at Kyangjing. In contrast, glacier ice averaged –16‰ with a standard deviation of ±2.3‰. Glacier ice values were similar even though they were collected from both Lirung and Langtang Glaciers at different elevations, but always in the ablation zone. Lirung Glacier outflow and supraglacial water had the largest range in between the pre- and post-monsoon periods, with median values changing by –5.1‰ and –7.0‰, respectively. Khimsung Glacier outflow median values also became depleted, changing by –2.1‰. The smallest magnitude of change in $\delta^{18}O$ between the seasons was in the low-elevation groundwater samples (–1.0‰), suggesting they are well integrated over time.

Langtang River water samples from four synoptic surveys in three different years show consistent enrichment in $\delta^{18}O$ values with decreasing elevation (+0.9‰ per kilometre of elevation loss) and a coincident decrease in geochemical weathering products (Fig. 4). For example, calcium concentrations in Late May decreased from 691 μEq L^{-1} at the R5 site to 483 μEq L^{-1} at R1. These spatial patterns suggest that reacted waters are primarily generated from debris-covered glaciers and moraine seepage in the upper Langtang basin and they become diluted at lower elevations. The Late May synoptic survey stands out as having the lowest concentrations of calcium, magnesium, sodium and sulfate, and the most enriched $\delta^{18}O$ values in waters from the Langtang River.

High-frequency sampling of outflow from debris-free Khimsung Glacier and debris-covered Lirung Glacier showed distinct differences between their geochemistry and isotopic content. Khimsung isotopic tracers had a median $\delta^{18}O$ value of –13.8‰ and a d-excess median of 13.5‰ (Fig. 5). In contrast, the $\delta^{18}O$ values in Lirung Glacier outflow were enriched, with a $\delta^{18}O$ median of –10.4‰ and a d-excess median of 15.6‰. Values of $\delta^{18}O$ and d-excess were statistically different between the two glaciers' outflows ($p \ll 0.01$, $n_{Km} = 36$, $n_{Li} = 22$). For both sites, there was also a temporal change in the isotopic content. In the

https://doi.org/10.3189/2016AoG71A067 Published online by Cambridge University Press

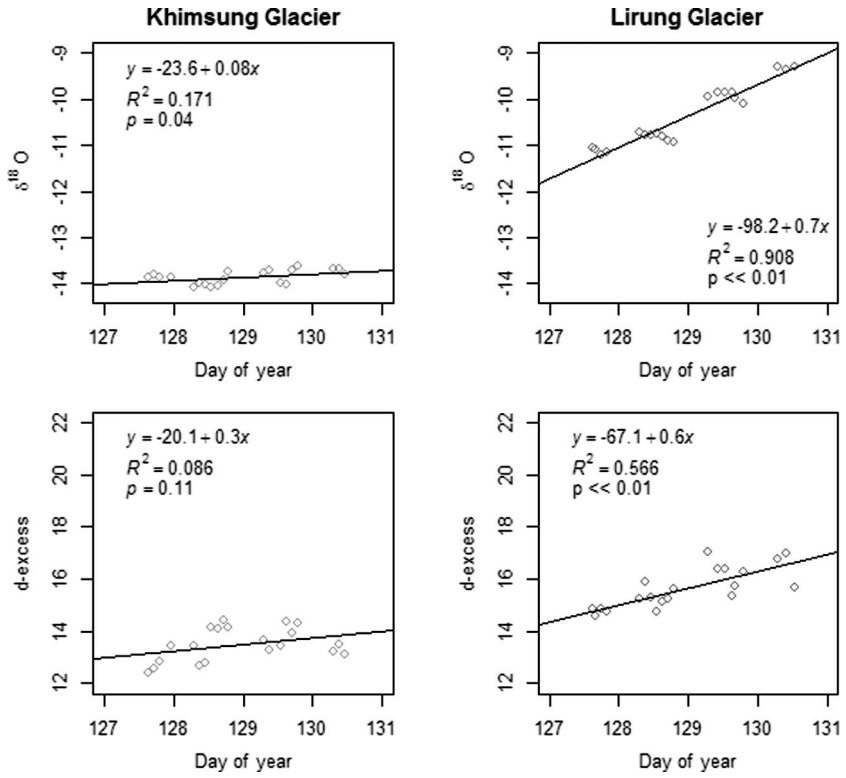

Fig. 5. Isotopic trends for bihourly sampling at debris-free Khimsung Glacier and debris-covered Lirung Glacier in May 2012.

Khimsung outflow, the increase in $\delta^{18}O$ values over time was small but statistically significant (slope = 0.08‰ d^{-1}, $R^2 = 0.171$, $p = 0.04$). In the Lirung outflow during the same period, the increasing trend in $\delta^{18}O$ was an order of magnitude greater (slope = 0.7‰ d^{-1}, $R^2 = 0.908$, $p \ll 0.01$). Deuterium-excess values behaved similarly.

Geochemical tracer concentrations for the debris-covered Lirung Glacier outflow were consistently higher and had less amplitude in their variation than the debris-free Khimsung Glacier outflow (Fig. 6). Calcium concentrations in Lirung outflow ranged from to 358 to 493 μEq L^{-1}, with an amplitude as small as 30 μEq L^{-1} d^{-1}. In Khimsung outflow the range of calcium values was 147–409 μEq L^{-1}, with a daily amplitude of at least 100 μEq L^{-1}. In contrast, minimum concentrations of sulfate from Lirung Glacier (200 μEq L^{-1}) were greater than maximum concentrations of sulfate from Khimsung Glacier (169 μEq L^{-1}). Chloride concentrations were much lower than the geochemical weathering products, <10 μEq L^{-1} at both sites. Generally, Khimsung Glacier outflow peaked in solute concentration for geochemical tracers during early morning, and minimum concentrations occurred in early to mid-afternoon. Diurnal

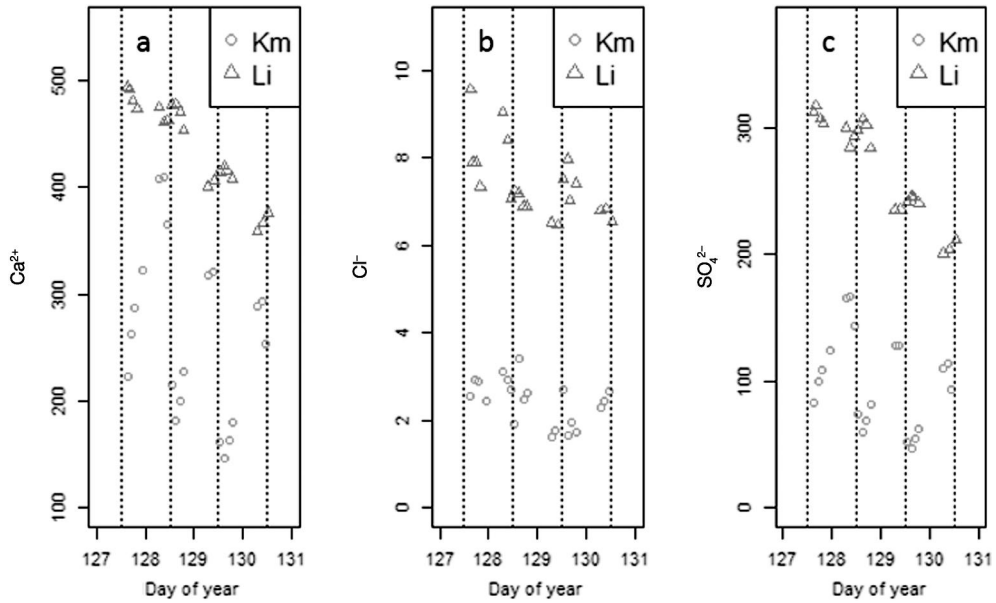

Fig. 6. Select geochemical tracer trends (μEq L^{-1}) for bihourly sampling at clean-ice Khimsung Glacier and debris-covered Lirung Glacier in May 2012. Vertical dotted lines mark noon for each day.

https://doi.org/10.3189/2016AoG71A067 Published online by Cambridge University Press

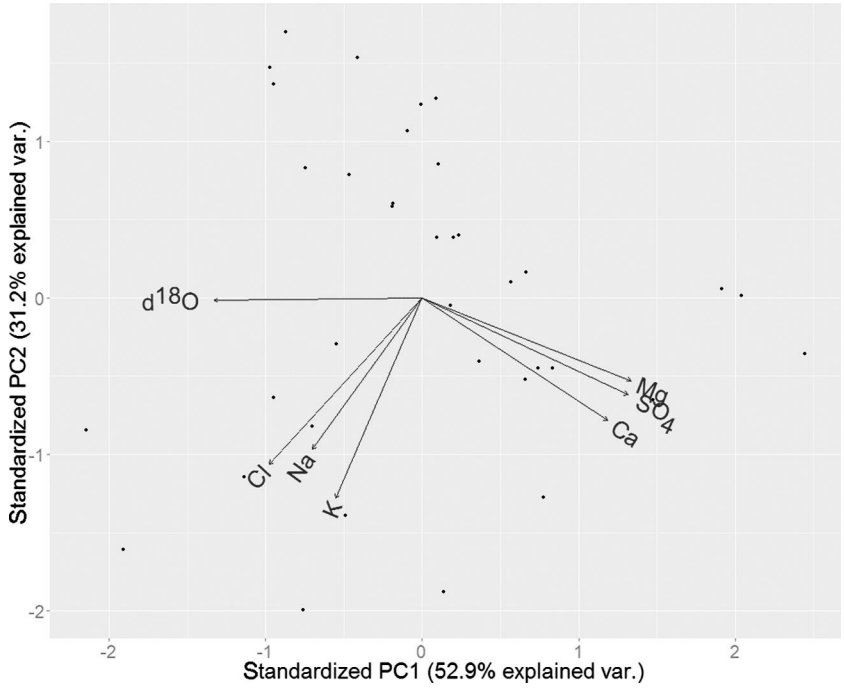

Fig. 7. Biplot of principal components 1 and 2, which together explain 84% of the variance in the dataset.

variations in solute concentrations for Lirung outflow were of smaller magnitudes.

4.2. Principal component analysis (PCA) and end-member mixing analysis (EMMA)

In order to investigate source waters and flow paths to the Langtang River we applied EMMA to all river samples collected over the four expeditions. We then plotted potential end-members (using the median when there was more than one sample) into the PCA space generated by the chemistry of the tracers in river water. Application of EMMA indicated that seven tracers were deemed conservative using the Hooper (2003) methodology (Ca^{2+}, Mg^{2+}, Na^{+}, K^{+}, Cl^{-}, SO_4^{2-} and $\delta^{18}O$). PCA found that two axes explained 84% of the variance in the chemistry of the tracers, indicating that three end-members contributed the majority of water to the Langtang River (Fig. 6). In general, we prefer that EMMA explain 90% or more of the variance (Liu and others, 2004). That two PCA axes explain only 84% of the variance suggests that there is a fourth unmeasured end-member.

A biplot of the principal components provides additional information on the tracers (Fig. 7). The biplot indicates that variance in $\delta^{18}O$ values is explained by the first principal component and is independent of the geochemical tracers. Calcium, magnesium and sulfate are correlated, which suggests these solutes are derived from a geochemical weathering source and that they are indicative of reacted waters. Sodium and chloride are also correlated, which

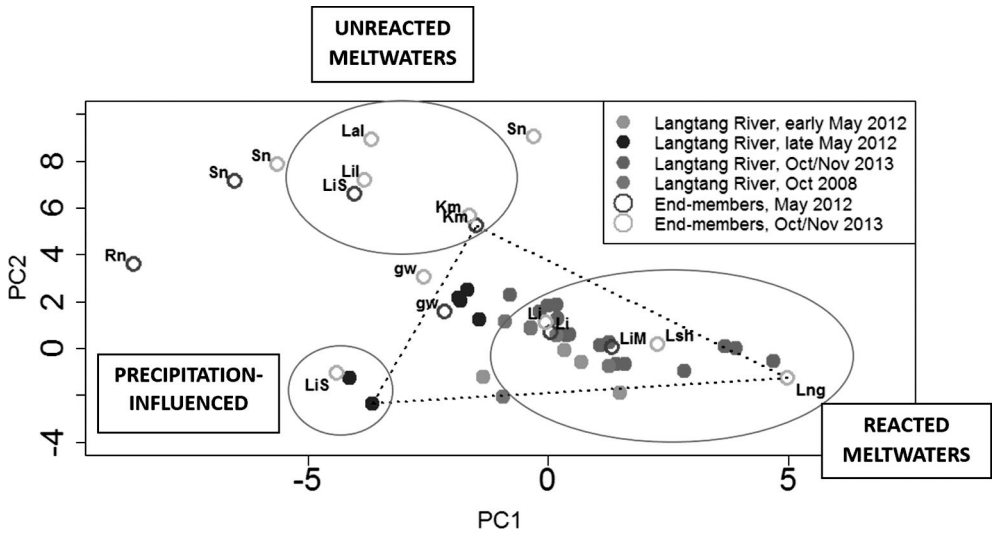

Fig. 8. EMMA results for three seasons of Langtang Valley water samples. Unreacted meltwaters generally have low calcium, magnesium and sulfate values but elevated sodium and chloride. Reacted meltwaters are characterized by elevated calcium, magnesium and sulfate. The plot region interpreted as precipitation-influenced has uniquely elevated sodium and chloride concentrations as well as high concentrations of calcium, magnesium and sulfate.

https://doi.org/10.3189/2016AoG71A067 Published online by Cambridge University Press

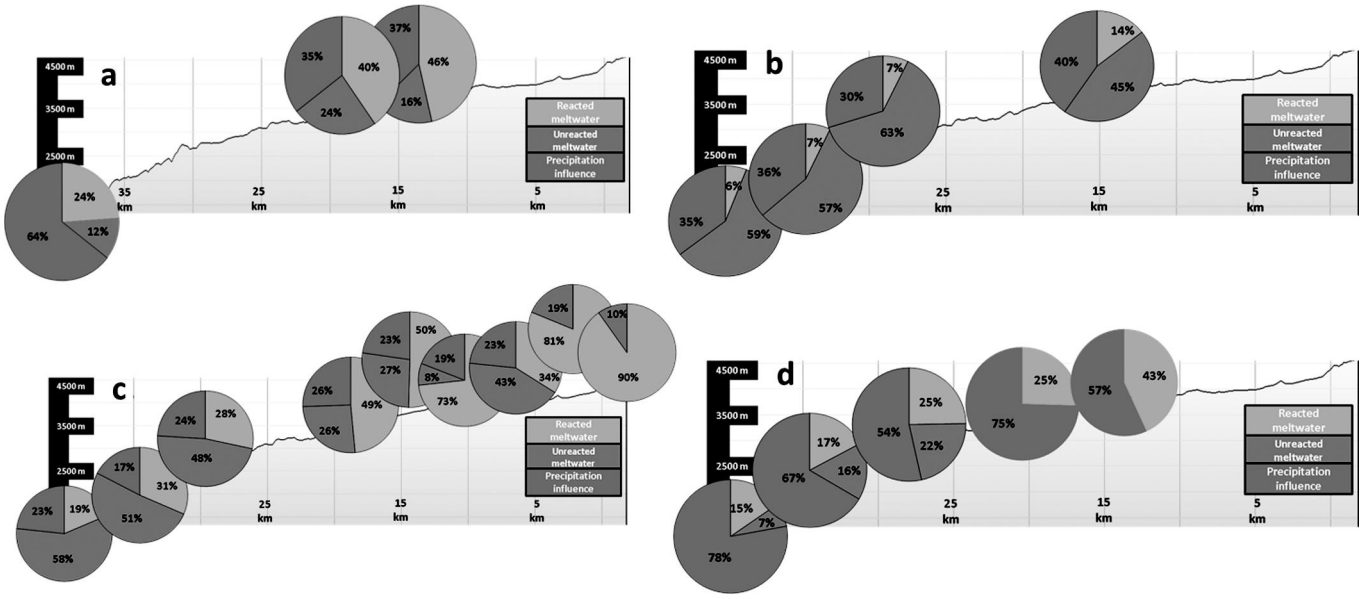

Fig. 9. EMMA hydrograph separation results for four synoptic surveys: (a) Early May 2012, (b) Late May 2012, (c) October 2013 and (d) November 2008. Blue is proportion of flow attributed to reacted water, red represents unreacted water, and green represents what we interpret as precipitation influence. Right to left on *x*-axis is distance downstream from the Langtang Glacier terminus (13× vertical exaggeration).

indicates that precipitation is the primary source of these solutes. These two sets of tracers help differentiate reacted and unreacted waters. Potassium is correlated with sodium and chloride, but is known to be influenced by biological controls (Likens and others, 1994) and has the lowest correlation coefficient of all the tracers.

When the seven geochemical and isotopic tracers were considered in EMMA, the end-member samples clustered in two main groups (Fig. 8). At the upper left of the EMMA plot, the cluster includes ice samples from Lirung and Langtang Glaciers, and outflow at the terminus of Khimsung Glacier. Given their low concentrations of geochemical weathering products, these samples are inferred to be unreacted meltwaters. Precipitation samples plot on the periphery of this cluster. On the right side of the plot, samples of outflow from the three debris-covered glaciers (Langtang, Lirung and Langshisha), and Lirung moraine seepage all contain elevated concentrations of geochemical weathering products and are interpreted to be reacted meltwater. Lirung supraglacial water plots with the unreacted samples in the pre-monsoon, and alone in the lower left in the post-monsoon. Neither Lirung nor Khimsung Glacier outflow samples vary in their PCA characterization between the pre-monsoon and post-monsoon time periods.

The points that most tightly bound the data cloud of river water samples are Langtang Glacier outflow, Khimsung Glacier outflow, and a Langtang River water sample from Late May 2012 collected at the DHM gauging station (site R4 in Fig. 1). Based on their chemistry profiles, the Langtang Glacier outflow represents reacted meltwater while the Khimsung Glacier outflow is representative of unreacted meltwater. The Late May river sample on the lower left had a sodium concentration 20% higher than the median for river samples (129 $\mu Eq\,L^{-1}$ vs 110 $\mu Eq\,L^{-1}$), and a chloride concentration four times higher than the river sample median (49 $\mu Eq\,L^{-1}$ vs 12 $\mu Eq\,L^{-1}$). The sodium and chloride values are similar to those measured in the rain samples (Fig. 3). The sample had calcium, magnesium, potassium and sulfate concentrations higher than rain but comparable to Lirung Glacier outflow, which has a reacted-water solute profile. Given that this combination of elevated solutes is associated with both rain and a reacted-water profile, the sample is interpreted to be influenced by pre-monsoon precipitation and subsurface routing. It was thus used as a proxy to represent a precipitation-influenced end-member that we hypothesize our dataset is missing.

In the EMMA analysis, the six Late May samples plot to the left of the other synoptic surveys and furthest from the reacted-water end-member (Fig. 8). The November 2008 samples and Early May 2012 plot with the same general pattern towards the center of the triangle. Four of the October/November 2013 samples plot to the far right and these are sites which are located closest to Langtang Glacier (sites R6, R7, R8 and R9) at elevations higher than all the other samples.

4.3. Langtang River hydrograph separation

Using the chosen end-members to calculate composition of river water yields percent estimates of reacted meltwater, unreacted meltwater and precipitation-influenced water in the river (Table 2; Fig. 9). River samples plotting outside the bounding triangle were moved to the line using the methodology of Liu and others (2004). Based on EMMA results, at the lowest-elevation site (R1) reacted meltwater contributed >20% of discharge in Early May and October/November, and >15% in November 2008. These are the seasons closest to base flow. During Late May, estimates of reacted meltwater contribution declined to 0% and 6% for the two available samples, and unreacted meltwater and precipitation-influenced water became dominant. At the highest site sampled in all four surveys, R5, reacted meltwater dominated in the Early May samples (59% on 8 May and 46% on 10 May), but unreacted meltwater played a large role in Late May (45%). The Early May and Late May synoptic surveys were <3 weeks apart but show a strong shift towards snowmelt and rain influence.

https://doi.org/10.3189/2016AoG71A067 Published online by Cambridge University Press

Table 2. EMMA results for all Langtang River water samples

Langtang River sample location	Season*	Date	$\delta^{18}O$ value	Reacted meltwater	Unreacted meltwater	Precipitation-influenced
			‰	%	%	%
R1	EM12	11 May 2012	–13.19	24	12	64
R4	EM12	10 May 2012	–13.77	40	24	35
R5	EM12	10 May 2012	–14.43	46	16	37
R5	EM12	8 May 2012	–15	59	0	41
R1	LM12	20 May 2012	–11.83	6	59	35
R1	LM12	24 May 2012	–12.05	0	15	85
R2	LM12	20 May 2012	–12.14	7	57	36
R3	LM12	21 May 2012	–12.32	7	63	30
R4	LM12	22 May 2012	–12.47	0	0	100
R5	LM12	22 May 2012	–12.88	14	45	40
R1	A13	19 Oct 2013	–15.42	19	58	23
R2	A13	19 Oct 2013	–15.68	31	51	17
R3	A13	19 Oct 2013	–15.82	28	48	24
R3	A13	20 Oct 2013	–15.84	29	51	20
R4	A13	21 Oct 2013	–16.34	49	26	26
R5	A13	21 Oct 2013	–16.78	50	27	23
R7	A13	26 Oct 2013	–15.83	34	43	23
R8	A13	27 Oct 2013	–17.51	81	19	0
R8	A13	27 Oct 2013	–17.46	80	20	0
R9	A13	27 Oct 2013	–17.37	90	10	0
R6	A13	1 Nov 2013	–16.48	73	8	19
R4	A13	5 Nov 2013	–15.83	55	14	31
R5	A13	9 Nov 2013	–15.87	57	14	29
R3	A13	11 Nov 2013	–15.06	39	33	28
R3	A13	12 Nov 2013	–14.97	39	33	29
R2	A13	21 Nov 2013	–14.72	29	38	33
R3	A13	21 Nov 2013	–15.05	31	0	69
R4	A13	24 Nov 2013	–15.56	54	13	33
R1	A13	25 Nov 2013	–13.11	21	43	36
R2	A13	25 Nov 2013	–14.72	29	39	33
R3	A13	25 Nov 2013	–15.02	36	33	31
R1	N08	23 Oct 2008	–12.83	15	7	78
R2	N08	24 Oct 2008	–13.3	17	16	67
R3	N08	25 Oct 2008	–14	25	22	54
Between R3 and R4	N08	25 Oct 2008	–13.66	25	0	75
R5	N08	27 Oct 2008	–14.64	43	0	57

*EM12: Early May 2012; LM12: Late May 2012; A13: October–November 2013; N08: November 2008.

The EMMA solutions were evaluated by reproducing concentrations of all conservative tracers from the EMMA model and comparing them to the measured values, following the protocol in Williams and others (2006). In general, EMMA reproduced the measured concentrations well. For example, the R^2 values for magnesium, chloride and sulfate were all >0.90 with slopes near 1 (Fig. 10). The Pearson correlation coefficient was >0.92 for five tracers, and >0.79 for all seven tracers, agreements comparable to those found by Liu and others (2004) in a snowmelt-dominated alpine catchment. The difference of the means was <12% for all tracers.

5. DISCUSSION

Concentrations of calcium, sodium and chloride in the pre-monsoon snow samples are comparable to values found in snow from the northern and western Tibetan Plateau and attributed there to dust sources (Wake and others, 1994; Thompson and others, 2000). Solute concentrations in both pre- and post-monsoon snow samples are up to an order of magnitude higher than those reported in the Khumbu Valley (Marinoni and others, 2001), though spatial and temporal variability in precipitation solute concentrations, particularly in snow, is not well constrained in the region. Marine-sourced moisture, such as that arriving with the monsoon, is known to have elevated sodium and chloride concentrations (Junge and Werby, 1958). Snow sourced from the westerlies outside of the monsoon is expected to have lower concentrations of sodium and chloride, as is seen in both the pre- and post-monsoon snow samples relative to the pre-monsoon rain samples. Geologic bedrock in the valley is thought to be free of halite (Evans and others, 2004), leaving precipitation as the primary source of chloride in all samples. The depletion of $\delta^{18}O$ values in the post-monsoon precipitation relative to the pre-monsoon is generally associated with source moisture of lower temperatures. Values of $\delta^{18}O$ are known to be enriched during the monsoon relative to other times of year, in Kyangjing peaking at around –5‰ in early summer and becoming depleted to around –20‰ by early winter (Zhang and others, 2001).

The similarity between pre-monsoon and post-monsoon geochemistry for outflow at both Lirung and Khimsung Glaciers, despite depletion in $\delta^{18}O$ values, signifies that similar flow paths and residence times can generate indistinguishable solute concentrations. The increasing

https://doi.org/10.3189/2016AoG71A067 Published online by Cambridge University Press

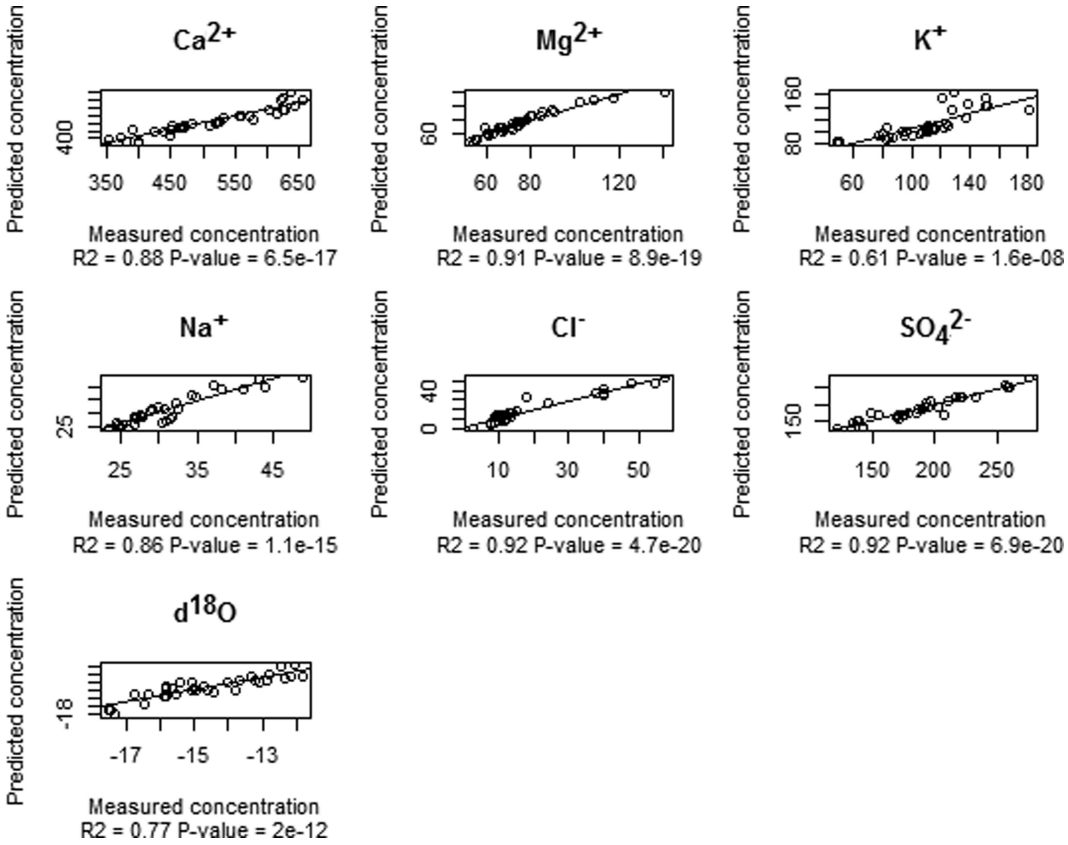

Fig. 10. Tracer concentrations (μEq L^{-1} and ‰) predicted using two principal components versus tracer concentrations measured in each Langtang River sample.

trend of $\delta^{18}O$ and deuterium-excess values in debris-covered Lirung Glacier relative to debris-free Khimsung Glacier could be attributable to more melt/freeze episodes for the debris-covered glacier compared to the debris-free glacier (Taylor and others 2002; Williams and others 2006). The presence of debris, which alters albedo and insolation dynamics, is known to facilitate a higher number of melt/freeze cycles, which in turn can elevate d-excess and enrich the remaining ice by 2–3‰ in $\delta^{18}O$ (Steig and others, 1998), similar to the difference we see between Lirung and Khimsung Glacier outflow samples. Isotopic fractionation may also play a role, as the first meltwater to leave seasonal snowpack is the most depleted (Williams and others, 2009). Changes in $\delta^{18}O$ and d-excess values of Khimsung Glacier are small over the 3 day window, suggesting melt/freeze cycles and isotopic fractionation of snowpack do not play a strong role in the isotopic history of the debris-free glacier outflow.

The pattern of decreasing geochemical concentrations during the day in Khimsung Glacier outflow may be attributable to dilution by clean snow and ice melt when peak melting occurs in the middle of the day. While englacial or subglacial storage can create a lag between discharge maxima and solute concentration minima (Anderson and others, 2003), the correlation at Khimsung Glacier between dilution of solute concentrations and time of maximum melt suggests there is little lag and that daily snow/ice melt dilution drives the chemograph patterns. The smaller magnitude of diurnal variability in Lirung Glacier outflow suggests larger subglacial storage, which can mute the amplitude of chemistry trends. Less snow or ice melt could also reduce the variability in chemistry.

Our hypothesis of a transition from unreacted snowmelt dominance in the pre-monsoon to reacted meltwater dominance in the post-monsoon generally holds, since unreacted meltwater comprises the majority of flow in Late May and only at the three lowest-elevation sites in autumn 2013. Most other samples have a higher proportion of reacted meltwater than unreacted meltwater. While we expected solute concentrations to increase with distance downstream due to increasing contributions from groundwater, this did not hold true. Reacted waters generally decreased with decreasing elevation, demonstrating an unexpected yet prominent role of groundwater and debris-covered glacier outflow in the hydrology of the upper Langtang basin. This is in contrast to many alpine catchments, where concentrations of solutes increase with distance downstream (Liu and others, 2004, 2008; Williams and others, 2006). Sodium and chloride concentrations showed lower variability with elevation, likely because these solutes are primarily sourced from precipitation and not affected by the geochemical weathering that generates reacted waters preferentially at higher elevations. Concentrations of most solutes did not show a distinct pattern with respect to pre- and post-monsoon samples, and glacier outflow samples generally showed overlap in solute concentrations between the seasons. This supports a conceptual model of the basin where debris-covered glacier meltwater and subsurface routing of other sources is dominant throughout the non-monsoon season, instead of direct runoff of snowmelt and debris-free glacier melt.

The large chemical dilution and enrichment of water isotopes between the Early May 2012 and Late May 2012 Langtang River samples appears to be the result of

https://doi.org/10.3189/2016AoG71A067 Published online by Cambridge University Press

unreacted meltwaters, likely snowmelt, entering the hydrologic system at this time. During this time, discharge measured at the DHM gauge (R4) rose from 3.67 $m^3 s^{-1}$ at the beginning of May to 8.26 $m^3 s^{-1}$ by the end of the month. The precipitation-influenced end-member is not yet dominating discharge, as monsoon rains have not yet arrived and DHM recorded only 14.8 mm of precipitation at Kyangjing in May 2012.

Further partitioning of the end-members into groundwater, rain, snowmelt or glacier melt may be possible with improved spatial and temporal characterization of end-member chemistry. The small sample size of rain and snow presented here does show differences between the two in most geochemical tracers and in $\delta^{18}O$ values, but a more robust dataset is required to pursue this question.

Results for the November 2008 samples cannot be directly compared to two-component mixing model estimates obtained by Racoviteanu and others (2013) because there is no direct correspondence between that approach and EMMA. EMMA is able to resolve variations in hydrochemistry that $\delta^{18}O$ alone cannot. However, for the November 2008 samples at the R1, R3 and R4 sampling sites, Racoviteanu and others (2013) estimate 73%, 63% and 30% groundwater contributions using $\delta^{18}O$ as the sole tracer. Our results included precipitation-influenced estimates of 78%, 54% and 64%; and 7%, 22% and 0% unreacted meltwater at the same locations. The attribution of precipitation influence to November samples suggests rain routed through the subsurface with an extended residence time can maintain the solute and isotopic profile associated with our pre-monsoon rain samples.

On an annual basis, Ragettli and others (2015) found that in 2012/13, discharge at R4 was 40% snowmelt, 34% rainfall and 26% glacier melt. While they acknowledge that some portions of these contributions are being routed through the subsurface, they do not explicitly quantify groundwater. They also surmise that they may be underestimating groundwater storage and groundwater routing of water that bypasses the channel. When our synoptic surveys from the pre- and post-monsoon seasons are averaged, the estimate of precipitation influence at R4 is 31%, which is comparable to Ragettli and others' (2015) findings for annual rainfall contribution. Other estimates of current annual glacier melt contribution in the upper Langtang basin include 62% (Brown and others, 2014) and ~40% (Immerzeel and others, 2012). This wide range of glacier melt values (26–62%) in recent literature emphasizes the need to explore in greater depth residence times, debris-covered versus debris-free ice melt, and monsoon contributions to base flow.

The EMMA approach utilized here is able to partition the hydrograph to estimate unreacted-meltwater, reacted-meltwater and precipitation-influenced contributions to discharge of the Langtang River. It offers a plausible framework for seasonal shifts in the hydrology of the basin; however, results for individual samples must be considered in light of limitations. Variability in end-member composition and the spatial and temporal constraints on our characterization of end-members reduce confidence in the hydrograph separation results. Also confounding the mixing model estimates is the complexity in timing of the three end-members. They are all dependent on meteorological conditions – precipitation, temperature, and radiation – and response to changing weather may be rapid. A more robust consideration of meteorological conditions may help explain the range of estimates of unreacted and precipitation-influenced end-members. Further consideration of uncertainty could be pursued with methodology such as Bayesian Monte Carlo mixing models (Arendt and others, 2015) and combining those results with EMMA.

6. CONCLUSIONS

It is apparent that subsurface flow paths and groundwater storage play a role in the hydrology of glacierized catchments that is often ignored. The presence of debris or the flow of water through moraines gives end-members a reacted geochemical profile, and the concentration of solutes actually declines with decreasing elevation, contrary to what is found in most alpine catchments. Many of the reacted and unreacted end-members defined here are influenced by melt processes, making differentiation of glacier inputs from snow inputs difficult. However, the rapid transition seen from reacted meltwater dominance in Early May Langtang River samples to unreacted meltwater and precipitation influence in Late May coincides with a doubling of discharge at the outlet of the upper Langtang basin. The significant differences observed between outflow chemistry of debris-covered Lirung Glacier and debris-free Khimsung Glacier may provide an opportunity to further separate their individual contributions to river discharge.

EMMA results support a conceptual model of the Langtang River basin where reacted-water contributions from groundwater and debris-covered glaciers are prominent throughout much of the year, with the exception of the monsoon. Late-fall estimates for October–November 2013 samples attributed less than a third of discharge to precipitation influence as the system transitions towards reacted-water base flow late in the year. Since the summer monsoon dominates the influx of water into the catchment and the regolith of the glaciated upper basin has high porosity, groundwater storage and residence time play an important role in the hydrology of the catchment. Understanding groundwater dynamics deserves additional attention in work examining the hydrology of high-alpine catchments in High Mountain Asia. Neither river water nor end-members from the monsoon are characterized here, but investigation of hydrochemistry in the summer season is warranted. Such characterizations and further applications of EMMA may offer additional insight into the source waters and flow paths that control Langtang River discharge and seasonality.

ACKNOWLEDGEMENTS

Support for this research came from US Agency for International Development (USAID) Cooperative Agreement AID-OAA-A-11-00045. Funding for A. Wilson was supported in part by a NASA Earth and Space Science Fellowship and the University of Colorado Department of Geography Adam Kolff Memorial Scholarship. Funding for M. Williams was supported in part by a US National Science Foundation grant to the Niwot Ridge Long-Term Ecological Research program. R. Kayastha was supported in part by a PEER award from USAID. Many thanks to DHM and the Cryosphere Monitoring Project, Kathmandu University, for the DHM discharge and precipitation data. Thanks also to the International Centre for Integrated Mountain Development (ICIMOD) for assisting in coordination of field logistics, and to ETH Zürich, Inge Juszak and Sonika Shahi

https://doi.org/10.3189/2016AoG71A067 Published online by Cambridge University Press

for automatic sampling equipment and collection. The comments of two anonymous reviewers were very helpful in improving the paper, as were the comments of Chief Editor Graham Cogley.

REFERENCES

Ageta Y and Higuchi K (1984) Estimation of mass balance components of a summer-accumulation type glacier in the Nepal Himalaya. *Geogr. Ann. A.*, **66A**(3), 249–255 (doi: 10.2307/520698)

Andermann C, Longuevergne L, Bonnet S, Crave A, Davy P and Gloaguen R (2012) Impact of transient groundwater storage on the discharge of Himalayan rivers. *Nature Geosci.*, **5**(2), 127–132 (doi: 10.1038/ngeo1356)

Anderson SP, Longacre SA and Kraal ER (2003) Patterns of water chemistry and discharge in the glacier-fed Kennicott River, Alaska: evidence for subglacial water storage cycles. *Chem. Geol.*, **202**(3), 297–312 (doi: 10.1016/j.chemgeo.2003.01.001)

Arendt CA, Aciego SM and Hetland EA (2015) An open source Bayesian Monte Carlo isotope mixing model with applications in Earth surface processes. *Geochem. Geophys. Geosyst.*, **16**, 1274–1292 (doi: 10.1002/2014GC005683)

Baral P and 9 others (2014) Preliminary results of mass-balance observations of Yala Glacier and analysis of temperature and precipitation gradients in Langtang Valley, Nepal. *Ann. Glaciol.*, **55**(66), 9–14 (doi: 10.3189/2014AoG66A106)

Barnard PL, Owen LA, Finkel RC and Asahi K (2006) Landscape response to deglaciation in a high relief, monsoon-influenced alpine environment, Langtang Himal, Nepal. *Quat. Sci. Rev.*, **25**(17), 2162–2176 (doi: 10.1016/j.quascirev.2006.02.002)

Barthold FK, Wu J, Vaché KB, Schneider K, Frede H-G and Breuer L (2010) Identification of geographic runoff sources in a data sparse region: hydrological processes and the limitations of tracer-based approaches. *Hydrol. Process.*, **24**(16), 2313–2327 (doi: 10.1002/hyp.7678)

Bookhagen B (2012) Hydrology: Himalayan groundwater. *Nature Geosci.*, **5**(2), 97–98 (doi: 10.1038/ngeo1366)

Brown and 16 others (2014) An integrated modeling system for estimating glacier and snow melt driven streamflow from remote sensing and earth system data products in the Himalayas. *J. Hydrol.*, **519**, 1859–1869 (doi: 10.1016/j.jhydrol.2014.09.050)

Chalise SR, Kansakar SR, Rees G, Croker K and Zaidman M (2003) Management of water resources and low flow estimation for the Himalayan basins of Nepal. *J. Hydrol.*, **282**(1), 25–35 (doi: 10.1016/S0022-1694(03)00250-6)

Christophersen N and Hooper RP (1992) Multivariate analysis of stream water chemical data: the use of principal components analysis for the end-member mixing problem. *Water Resour. Res.*, **28**(1), 99–107 (doi: 10.1029/91WR02518)

Christophersen N, Neal C, Hooper RP, Vogt RD and Andersen S (1990) Modelling streamwater chemistry as a mixture of soilwater end-members: a step towards second-generation acidification models. *J. Hydrol.*, **116**(1), 307–320 (doi: 10.1016/0022-1694(90)90130-P)

Evans MJ, Derry LA and France-Lanord C (2004) Geothermal fluxes of alkalinity in the Narayani river system of central Nepal. *Geochem. Geophys. Geosyst.*, **5**(8), Q08011 (doi: 10.1029/2004GC000719)

Higuchi K (1993) Nepal–Japan cooperation in research on glaciers and climates of the Nepal Himalaya. *IAHS Publ.* 218 (Symposium at Kathmandu 1992 – *Snow and Glacier Hydrology*)

Hooper RP (2003) Diagnostic tools for mixing models of stream water chemistry. *Water Resour. Res.*, **39**(3) (doi: 10.1029/2002WR001528)

Hooper RP and Shoemaker CA (1986) A comparison of chemical and isotopic hydrograph separation. *Water Resour. Res.*, **22**(10), 1444–1454 (doi: 10.1029/WR022i010p01444)

Hooper RP, Christophersen N and Peters NE (1990) Modelling streamwater chemistry as a mixture of soilwater end-members: an application to the Panola Mountain catchment, Georgia, USA. *J. Hydrol.*, **116**(1), 321–343 (doi: 10.1016/0022-1694(90)90131-G)

Immerzeel WW, Van Beek LPH and Bierkens MFP (2010) Climate change will affect the Asian water towers. *Science*, **328**(5984), 1382–1385 (doi: 10.1126/science.1183188)

Immerzeel WW, Van Beek LPH, Konz M, Shrestha AB and Bierkens MFP (2012) Hydrological response to climate change in a glacierized catchment in the Himalayas. *Climatic Change*, **110**(3–4), 721–736 (doi: 10.1007/s10584-011-0143-4)

Inger S and Harris N (1993) Geochemical constraints on leucogranite magmatism in the Langtang Valley, Nepal Himalaya *J. Petrol.*, **34**(2), 345–368 (doi: 10.1093/petrology/34.2.345)

Johnsen SJ, Dansgaard W and White JWC (1989) The origin of Arctic precipitation under present and glacial conditions. *Tellus B*, **41**(4), 452–468 (doi: 10.1111/j.1600-0889.1989.tb00321.x)

Junge CE and Werby RT (1958). The concentration of chloride, sodium, potassium, calcium, and sulfate in rain water over the United States. *J. Meteorol.*, **15**(5), 417–425 (doi: 10.1175/1520-0469(1958)015<0417:TCOCSP>2.0.CO;2)

Kayastha RB, Takeuchi Y, Nakawo M and Ageta Y (2000) Practical prediction of ice melting beneath various thickness of debris cover on Khumbu Glacier, Nepal, using a positive degree-day factor. *IAHS Publ.* 264 (Workshop at Seattle 2000 – *Debris-Covered Glaciers*), 71–82

Kong Y and Pang Z (2012) Evaluating the sensitivity of glacier rivers to climate change based on hydrograph separation of discharge. *J. Hydrol.*, **434**, 121–129 (doi: 10.1016/j.jhydrol.2012.02.029)

La Frenierre J and Mark BG (2014) A review of methods for estimating the contribution of glacial meltwater to total watershed discharge. *Progr. Phys. Geogr.*, **38**(2), 173–200 (doi: 10.1177/0309133313516161)

Likens GE and 8 others (1994) The biogeochemistry of potassium at Hubbard Brook. *Biogeochemistry*, **25**(2), 61–125 (doi: 10.1007/BF00000881)

Liu F, Williams MW and Caine N (2004). Source waters and flow paths in an alpine catchment, Colorado Front Range, United States. *Water Resour. Res.*, **40**(9), W09401 (doi: 10.1029/2004WR003076)

Liu F, Bales RC, Conklin MH and Conrad ME (2008). Streamflow generation from snowmelt in semi-arid, seasonally snow-covered, forested catchments, Valles Caldera, New Mexico. *Water Resour. Res.*, **44**(12), W12443 (doi: 10.1029/2007WR006728)

Macfarlane AM (1993) Chronology of tectonic events in the crystalline core of the Himalaya, Langtang National Park, central Nepal. *Tectonics*, **12**(4), 1004–1025 (doi: 10.1029/93TC00916)

Marinoni A, Polesello S, Smiraglia C and Valsecchi S (2001) Chemical composition of fresh snow samples from the southern slope of Mt. Everest region (Khumbu-Himal region, Nepal). *Atmos. Environ.*, **35**(18), 3183–3190 (doi: 10.1016/S1352-2310(00)00488-X)

Motoyama H and Yamada T (1989) Hydrological observations of Langtang Valley, Nepal Himalayas during 1987 monsoon–postmonsoon season. *Bull. Glacier Res.*, **7**, 195–201

Nepal S, Krause P, Flügel WA, Fink M and Fischer C (2014). Understanding the hydrological system dynamics of a glaciated alpine catchment in the Himalayan region using the J2000 hydrological model. *Hydrol. Process.*, **28**(3), 1329–1344 (doi: 10.1002/hyp.9627)

Pellicciotti F, Stephan C, Miles E, Herreid S, Immerzeel WW and Bolch T (2015) Mass-balance changes of the debris-covered glaciers in the Langtang Himal, Nepal, from 1974 to 1999. *J. Glaciol.*, **61**(226), 373–386 (doi: 10.3189/2015JoG13J237)

Poage MA and Chamberlain CP (2001) Empirical relationships between elevation and the stable isotope composition of precipitation and surface waters: considerations for studies of

paleoelevation change. *Am. J. Sci.*, **301**(1), 1–15 (doi: 10.2475/ajs.301.1.1)

Racoviteanu AE, Armstrong R and Williams MW (2013) Evaluation of an ice ablation model to estimate the contribution of melting glacier ice to annual discharge in the Nepal Himalaya. *Water Resour. Res.*, **49**(9), 5117–5133 (doi: 10.1002/wrcr.20370)

Ragettli S and 6 others (2015). Unraveling the hydrology of a Himalayan catchment through integration of high resolution in situ data and remote sensing with an advanced simulation model. *Adv. Water Res.*, **78**, 94–111 (doi: 10.1016/j.advwatres.2015.01.013)

Sakai A, Nakawo M and Fujita K (1998) Melt rate of ice cliffs on the Lirung Glacier, Nepal Himalayas, 1996. *Bull. Glacier Res.*, **16**, 57–66

Schramm JM, Weidinger JT and Ibetsberger HJ (1998) Petrologic and structural controls on geomorphology of prehistoric Tsergo Ri slope failure, Langtang Himal, Nepal. *Geomorphology*, **26**(1), 107–121 (doi: 10.1016/S0169-555X(98)00053-1)

Steig EJ, Fitzpatrick JJ, Potter N Jr and Clark DH (1998). The geochemical record in rock glaciers. *Geogr. Ann. A*, **80**(3–4), 277–286 (doi: 10.1111/j.0435-3676.1998.00043.x)

Sueker JK, Clow DW, Ryan JN and Jarrett RD (2001). Effect of basin physical characteristics on solute fluxes in nine alpine/subalpine basins, Colorado, USA. *Hydrol. Process.*, **15**(14), 2749–2769 (doi: 10.1002/hyp.265)

Taylor S, Feng X, Williams M and McNamara J (2002). How isotopic fractionation of snowmelt affects hydrograph separation. *Hydrol. Process.*, **16**(18), 3683–3690 (doi: 10.1002/hyp.1232)

Thompson LG, Yao T, Mosley-Thompson E, Davis ME, Henderson KA and Lin PN (2000) A high-resolution millennial record of the South Asian monsoon from Himalayan ice cores. *Science*, **289**(5486), 1916–1919 (doi: 10.1126/science.289.5486.1916)

United Nations Environmental Program (UNEP) and World Glacier Monitoring Service (WGMS) (2008) *Global glacier change: facts and figures, section 6.9: Regional glacier changes in Central Asia*. UNEP, Zürich http://www.grid.unep.ch/glaciers/

Wagnon P and 10 others (2007) Four years of mass balance on Chhota Shigri Glacier, Himachal Pradesh, India, a new benchmark glacier in the western Himalaya. *J. Glaciol.*, **53**(183), 603–611 (doi: 10.3189/002214307784409306)

Wake CP, Dibb JE, Mayewski PA, Zhongqin L and Zichu X (1994). The chemical composition of aerosols over the eastern Himalayas and Tibetan Plateau during low dust periods. *Atmos. Environ.*, **28**(4), 695–704 (doi: 10.1016/1352-2310(94)90046-9)

Williams MW, Knauf M, Caine N, Liu F and Verplanck PL (2006). Geochemistry and source waters of rock glacier outflow, Colorado Front Range. *Permafrost Periglac. Process.*, **17**(1), 13–33 (doi: 10.1002/ppp.535)

Williams MW, Seibold C and Chowanski K (2009). Storage and release of solutes from a subalpine seasonal snowpack: soil and stream water response, Niwot Ridge, Colorado. *Biogeochemistry*, **95**(1), 77–94 (doi: 10.1007/s10533-009-9288-x)

Zemp M, Hoelzle M and Haeberli W (2009). Six decades of glacier mass-balance observations: a review of the worldwide monitoring network. *Ann. Glaciol.*, **50**(50), 101–111 (doi: 10.3189/172756409787769591)

Zhang X, Masayoshi N, Fujita K, Yao T and Han J (2001). Variation of precipitation $\delta^{18}O$ in Langtang Valley Himalayas. *Sci. China D*, **44**(9), 769–778 (doi: 10.1007/BF02907089)

https://doi.org/10.3189/2016AoG71A067 Published online by Cambridge University Press